POLITECNICO DI TORINO
Repository ISTITUZIONALE

Effect of heat treatment on microstructural evolution of additively manufactured Inconel 718 and cast alloy

Original
Effect of heat treatment on microstructural evolution of additively manufactured Inconel 718 and cast alloy / Saboori, A., Marchese, G., Aversa, A., Bassini, E., Mazzucato, F., Valente, A., Lombardi, M., Ugues, D., Biamino, S., Fino, P.. - CD-ROM. - (2019), pp. 1-6. (EuroPM 2019 Maastricht 13-17 October 2019).

Availability:
This version is available at: 11583/2766014 since: 2019-11-11T12:28:31Z

Publisher:
European Powder Metallurgy Association (EPMA)

Published
DOI:

Terms of use:

This article is made available under terms and conditions as specified in the corresponding bibliographic description in the repository

Publisher copyright

(Article begins on next page)

21 November 2026

Manuscript refereed by Chairman Name (Company, Country)

Effect of heat treatment on microstructural evolution of additively manufactured Inconel 718 and cast alloy

Abdollah Saboori[1], Giulio Marchese[1], Alberta Aversa[1], Emilio Bassini[1], Federico Mazzucato[2], Anna Valente[2], Mariangela Lombardi[1], Daniele Ugues[1], Sara Biamino[1], Paolo Fino[1]

[1] Department of Applied Science and Technology, Politecnico Di Torino, Corso Duca degli Abruzzi 24, 10129 Torino, Italy

[2] SUPSI ISTePS-Institute of Systems and Technologies for the Sustainable Production, Galleria 2, Manno, Switzerland

Abstract

Additive manufacturing (AM) processes facilitate the fabrication of complex shape metallic components directly from Computer-Aided Design models, which may be challenging to be produced using conventional manufacturing technologies. However, it is revealed that additively manufactured components usually have non-equilibrium microstructures. Thus, post-built heat treatments are recommended for AM components to achieve homogenous microstructures. In this study, the effects of solution annealing and ageing treatments on the microstructure evolution of Inconel 718 alloy processed by laser powder bed fusion (LPBF) and directed energy deposition (DED) processes are compared with those produced by casting. Microstructural characterization techniques including OM, SEM/EDS analysis were employed on AM and cast components to obtain more information regarding the microstructure and phase evolution during these heat treatments. These microstructural studies demonstrate that the starting microstructure could play a key role in the microstructural evolution during the heat treatment of Inconel 718 alloy.

Keyword: Inconel 718, Casting, Laser Powder Bed Fusion, Directed Energy Deposition, Heat treatment

1. Introduction:

Inconel 718 (IN718), a Ni-Cr-Fe austenite (γ) superalloy, has been widely used in various applications such as turbine blades, combustion chambers and nuclear reactors because of its excellent oxidation and corrosion resistance, as well as unique creep properties [1]. In general, IN718 superalloy has been produced and used in wrought, cast and powder metallurgy forms [2,3]. As a core element of the hot-end structural components, IN718 can retain its superior mechanical properties in a broad range of temperatures by virtue of solid–solution strengthening and precipitation strengthening [1,4]. Thus, the appropriate selection of a specific production technique for a given component depends on geometrical complexity, production quantity and cost, material and required mechanical properties. Based on these issues, the different manufacturing techniques offer certain disadvantages and advantages. Casting technology can provide high productivity and freedom in size of parts, however, owing to the high hardness and low thermal conductivity features of IN718, it is challenging to apply conventional machining methods as a consequence of tool over-wear and poor workpiece surface integrity [5]. Therefore, the application of the novel production technologies like Additive Manufacturing (AM) technologies is necessary to the net-shape manufacturing of IN718 components with complex shape and high performances. In fact, AM technologies offer a wide freedom in geometrical design

© European Powder Metallurgy Association (EPMA)

whereas, the production quantity and the dimension of the part are limiting their applications [6,7]. Moreover, repeated rapid heating and cooling during AM processes can generate a steep thermal gradient which results in the formation of high residual stress inside the IN718 parts produced via these technologies. It is reported that this residual stress will cause distortionsfor the as-built AM samples and thus further thermal treatment is necessary to relieve the residual stresses and enable the precipitation of strengthening phases and [8]. One of the most important heat treatments to modify the phase composition of as-built components is solution-ageing treatment. The first step allows the dissolution of phases as well as chemical segregations while the ageing treatment promotes the formation of γ' and γ'' phases in order to strengthening the alloy. According to previous works, also deleterious Laves $(Ni,Fe,Cr)_2(Nb,Mo,Ti)$ phase and δ (Ni_3Nb) phase may form. It is reported that since the Laves and δ phase are incoherent phases, do not contribute to the strengthening of IN718 alloy. Moreover, precipitation of these phases deplete the available Nb for the precipitation of the strengthening phases (γ' and γ'' phases) and even decrease ductility [9]. Therefore, in order to improve the mechanical properties of IN718 samples, it is mandatory to properly optimize their heat treatment, both solution and ageing.

In the literature, there are several works on the optimization of process parameters of Directed energy Deposition (DED) and Laser Powder Bed Fusion (LPBF) process to produce fully dense components [10–12]. However, to date, notwithstanding the reports that come out around the microstructural evolution during various process parameters, there are rather limited investigations on a direct comparison of how the different starting microstructures respond to the standard solution-ageing heat treatment [13]. Therefore, this work aims to study the effects of solution-ageing treatment on the microstructure evolution of IN718 alloy produced via various production processes such as casting, LPBF and DED process.

2. Materials and methods:

The samples processed by LPBF, DED and casting processes were heat-treated with the following schedule in this work; a solution heat treatment, a first ageing and second ageing. These steps were performed at 982, 720 and 620 °C with a dwell time of 1h, 8h and 8h, respectively (Figure 1). For each step, the heating rate was set at 20°C/min. All the heat treatments were performed in a low-pressure horizontal furnace TAV MINIJET HP S/N 235 with vacuum level set at 10^{-2} mbar. All the samples were inserted at the same time in the furnace, independently by the manufacturing route and progressively removed after each heat treatment step in order to assess any alteration brought by solution, first ageing and second ageing, respectively. The microstructure of as-produced and three chosen heat treated IN718 specimens were observed after the standard metallography of specimens. For this reason, the samples produced by AM technologies were cut parallel to the building direction and then ground and polished down to 1 μm using SiC waterproof abrasive paper and Dimond paste following by etching using Kalling's No.2 solution (5 g $CuCl_2$ in 100 ml HCl and 100 ml CH_3CH_2OH) for 30 s. Thereafter, the microstructures were revealed using an optical microscope (OM Leica DMI 5000M) and scanning electron microscope (SEM, Phenom).

© European Powder Metallurgy Association (EPMA)

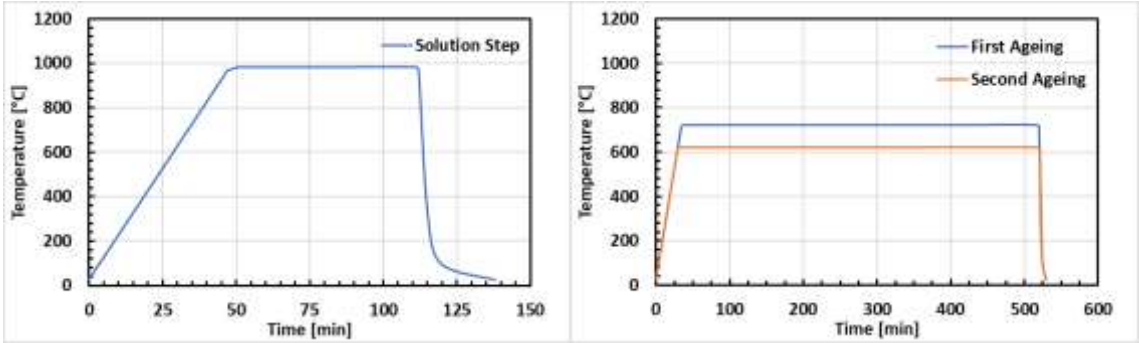


Figure 1 Core Temperature vs time measured in a dummy sample placed among the samples which were actually heat treated.

3. Results and discussion:

The microstructure of as-cast, as-built LPBF and DED samples are shown in Figure 1 (a-c). As it can be seen, the as-cast microstructure is characterized by equiaxed grains with austenite dendrites consist of some brittle intermetallic compounds (Laves eutectic phase) and Nb-rich carbides in the interdendritic regions (yellow arrows in Insert in Figure1(a)). Whereas, the cross-section of as-built LPBF and DED samples are characterized by columnar dendrite grains growing along the building direction and arc-shape melt pools that formed due to the Gaussian distribution of laser beam energy and wetting properties of the liquid, solid interface. Some fine secondary dendrite structures with identical growth orientation stretched over some adjacent layers can also be observed in AM samples. In contrast to the dark austenite matrix, small white phases can be seen along the interdendritic boundaries. They are identified as the laves phase, some minor Nb-rich carbides as well as segregated elements formed during the rapid solidification. In fact, rapid solidification of each thin layer results in the directional grain growth, microsegregation of high concentration refractory elements such as Nb and Mo and formation of non-equilibrium phases, including carbides, Laves phases or sub-micrometric segregation and consequently the precipitation of the strengthening γ′ and γ″ phases is inhibited [14].

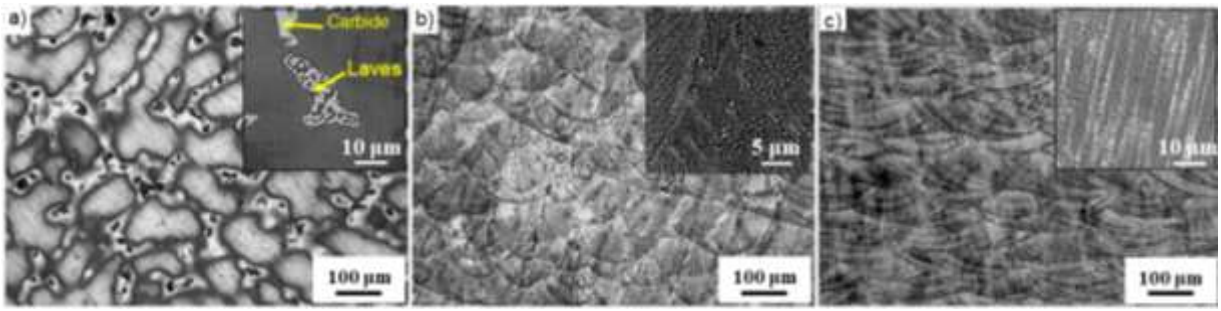


Figure 2 OM micrograph of IN718 alloy in (a) as-cast, (b) as-built LPBF, (c) as-built DED conditions.

Moreover, it seems that the size of Laves phase in LPBF and DED samples is much smaller than that of conventional casting IN718, which makes the phase easily to be dissolved into the matrix. This different behaviour in the segregation can be related to the solidification rate so that in AM processes, this phenomena can be prevented completely. In comparison to the LPBF, the size of laves phase in the DED sample seems coarser which is directly correlated to its lower solidification rate.

© European Powder Metallurgy Association (EPMA)

Figure 3 shows the as-solutionized microstructure of IN718 alloy produced by casting, LPBF and DED. In general, as mentioned earlier the goal of solution treatment is to homogenize the chemical elements dissolving segregations and possible phases in order to prepare the material for the double ageing which is going to precipitate the different sizes/shapes of fine γ' and γ'' phases. As can be seen in Figure 3, a fraction of the Laves phase were dissolved in the matrix, and a lower quantity of this phase can be seen in all samples. However, Laves phase seems to be richer and larger in the cast samples. Nonetheless, the microstructures imply that the solution temperature was not high enough to dissolve completely all the Laves phase and also to start the recrystallization in the AM samples.

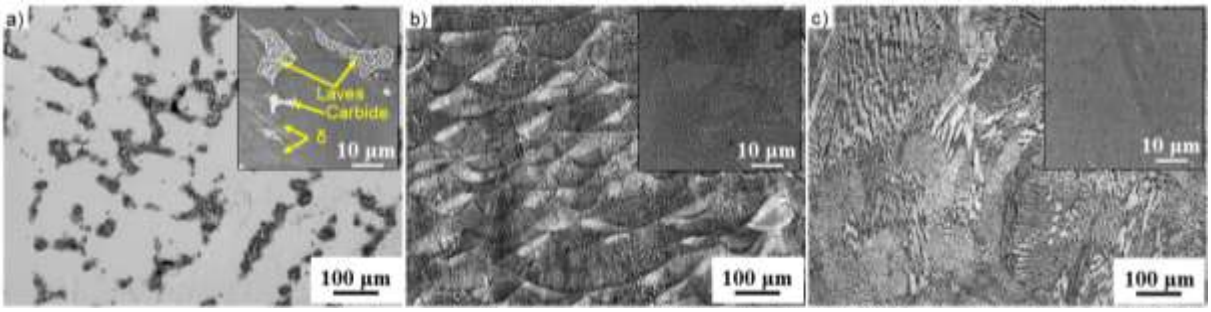


Figure 3 OM/SEM micrograph of IN718 alloy produced by (a) casting, (b) LPBF, (c) DED, after solution treatment.

Figure 4 shows the OM microstructure of IN718 produced by casting, LPBF and DED after solution and double ageing heat treatment. As can be seen in this figure, in the casted specimens there is still an high level of Laves phase and δ phase with needle-like structure at the interdendritic areas. Since the δ phase needs less Nb with respect to the Laves phase, the transformation indicates that the as-deposited high concentration of Nb at interdendritic regions has been partially dissolved into the matrix. Moreover, it is found that there is some trace of the Laves phase, even after solution-ageing heat treatment, that confirms again that 980°C as the solution treatment is not high enough to dissolve the Laves phase completely. Moreover, in the case of AM samples, the layer interface regions can still be revealed after the solution-ageing heat treatment. According to literature, this microstructural feature can be eliminated through the homogenization treatment at a higher temperature (typically 1065 °C for 1 h), which results in the recrystallization of grains and consequently, more isotropic appearance [13].

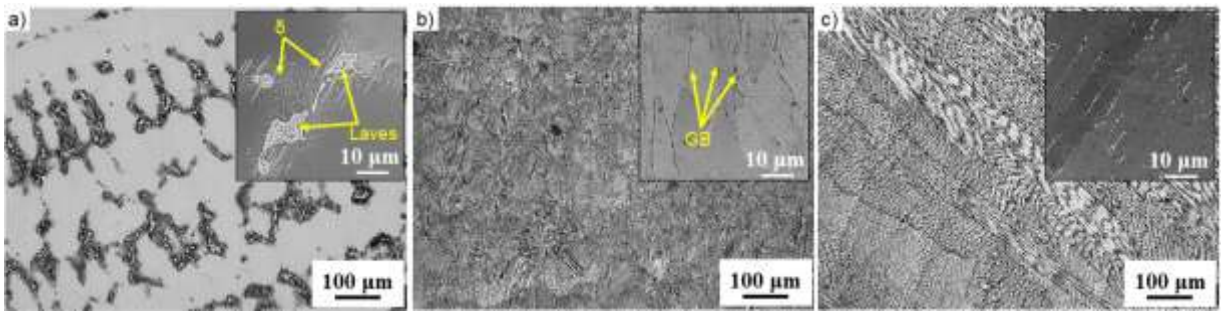


Figure 4 OM/SEM micrograph of IN718 alloy produced by (a) casting, (b) LPBF, (c) DED, after Aging 2.

Figure 5 (a-f) compares the microstructure of samples produced via casting, LPBF and DED, after solution treatment followed by double ageing. It is apparent from this Figure that the size of precipitates is very fine compared to the casted sample. The majority of the phases are δ phases as evident by their acicular shapes and increment of Nb in the EDS maps. Furthermore, the majority of

© European Powder Metallurgy Association (EPMA)

the precipitates are located at the grain boundary so that in the SLM sample it seems the grain boundaries are decorated with the precipitates, mainly Laves and δ phases. The high concentration of intergranular precipitates derived from the presence of segregated elements within the grain boundaries. In this Figure, the EDS analysis corresponding to the points (I) and (II) are shown.

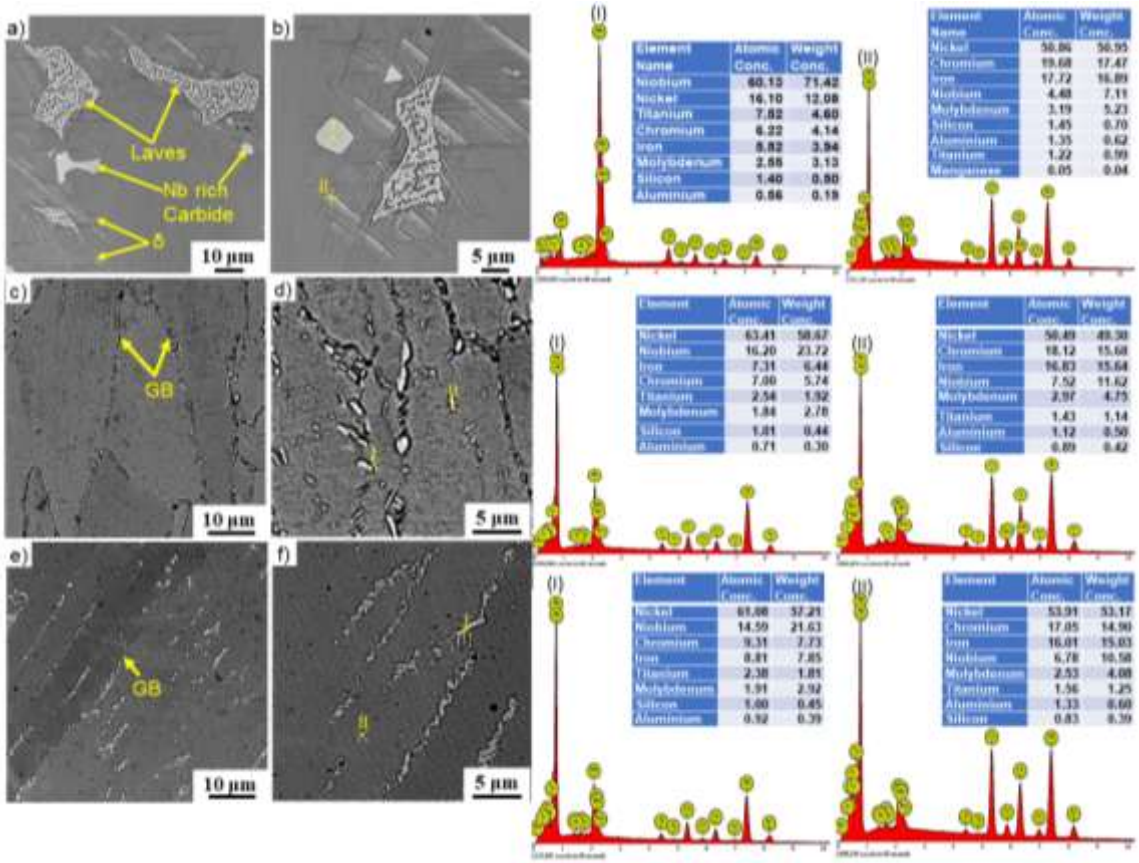


Figure 5 SEM/EDS analysis of (a-b) LPBF, (c-d) DED samples after solution-double ageing heat treatment (EDS (I) and (II) are corresponding EDS analysis to the points of (I) and (II))

However, it should be noted that, according to literature, even if the precipitation γ′ and γ″ phases starts during the ageing step, owing to their dimensions that would be in the nanoscale needs more deep characterization via FESEM and TEM [14].

Conclusion:

In this work, the correlation between the starting microstructure and the solution and double ageing treatment of the IN718 superalloy were investigated. The main findings can be summarized as follows:

- The as-built AM IN718 samples have columnar grains with a dendritic structure including numbers of fine Laves phases or segregation of Nb and Mo in the interdendritic region.
- Driven by ultra-high temperature gradient and ultra-fast cooling rate during AM process compared with the conventional casting process, the fine, nearly directional solidified grain including very fine Laves phase /Nb-rich carbide is formed that change the kinetics of solution treatment.
- 980°C as the solution treatment is not high enough to dissolve the harmful Laves and Carbide phases, but starts an initial chemical homogenization.
- In the case of AM samples, the solution-double ageing process does not result in recrystallization, and thus, the layer interface regions still present after the heat treatment.

© European Powder Metallurgy Association (EPMA)

Acknowledgements

The authors would like to acknowledge the European research project belonging to the Horizon 2020 research and innovation programme; 4D Hybrid—Novel ALL-IN-ONE machines, robots and systems for affordable, worldwide and lifetime Distributed 3D hybrid manufacturing and repair operations (grant agreement no.723795).

References

1. Jia, Q.; Gu, D. Selective laser melting additive manufacturing of Inconel 718 superalloy parts: Densification, microstructure and properties. *J. Alloys Compd.* **2014**, *585*, 713–721, doi:https://doi.org/10.1016/j.jallcom.2013.09.171.
2. Zheng, L.; Schmitz, G.; Meng, Y.; Chellali, R.; Schlesiger, R. Mechanism of Intermediate Temperature Embrittlement of Ni and Ni-based Superalloys. *Crit. Rev. Solid State Mater. Sci.* **2012**, *37*, 181–214, doi:10.1080/10408436.2011.613492.
3. Kuo, C.-M.; Yang, Y.-T.; Bor, H.-Y.; Wei, C.-N.; Tai, C.-C. Aging effects on the microstructure and creep behavior of Inconel 718 superalloy. *Mater. Sci. Eng. A* **2009**, *510–511*, 289–294, doi:https://doi.org/10.1016/j.msea.2008.04.097.
4. González-Fernández, L.; del Campo, L.; Pérez-Sáez, R. B.; Tello, M. J. Normal spectral emittance of Inconel 718 aeronautical alloy coated with yttria stabilized zirconia films. *J. Alloys Compd.* **2012**, *513*, 101–106, doi:https://doi.org/10.1016/j.jallcom.2011.09.097.
5. Izquierdo, B.; Plaza, S.; Sánchez, J. A.; Pombo, I.; Ortega, N. Numerical prediction of heat affected layer in the EDM of aeronautical alloys. *Appl. Surf. Sci.* **2012**, *259*, 780–790, doi:https://doi.org/10.1016/j.apsusc.2012.07.124.
6. Saboori, A.; Gallo, D.; Biamino, S.; Fino, P.; Lombardi, M. An overview of additive manufacturing of titanium components by directed energy deposition: Microstructure and mechanical properties. *Appl. Sci.* **2017**, *7*, doi:10.3390/app7090883.
7. Saboori, A.; Tusacciu, S.; Busatto, M.; Lai, M.; Biamino, S.; Fino, P.; Lombardi, M. Production of Single Tracks of Ti-6Al-4V by Directed Energy Deposition to Determine the Layer Thickness for Multilayer Deposition. *J. Vis. Exp.* **2018**, *2018*, e56966, doi:doi:10.3791/56966.
8. Zhang, D.; Niu, W.; Cao, X.; Liu, Z. Effect of standard heat treatment on the microstructure and mechanical properties of selective laser melting manufactured Inconel 718 superalloy. *Mater. Sci. Eng. A* **2015**, *644*, 32–40, doi:https://doi.org/10.1016/j.msea.2015.06.021.
9. Rao, G. A.; Kumar, M.; Srinivas, M.; Sarma, D. S. Effect of standard heat treatment on the microstructure and mechanical properties of hot isostatically pressed superalloy inconel 718. *Mater. Sci. Eng. A* **2003**, *355*, 114–125, doi:https://doi.org/10.1016/S0921-5093(03)00079-0.
10. Bennett, J. L.; Wolff, S. J.; Hyatt, G.; Ehmann, K.; Cao, J. Thermal effect on clad dimension for laser deposited Inconel 718. *J. Manuf. Process.* **2017**, *28*, 550–557, doi:https://doi.org/10.1016/j.jmapro.2017.04.024.
11. Lu, Y.; Wu, S.; Gan, Y.; Huang, T.; Yang, C.; Junjie, L.; Lin, J. Study on the microstructure, mechanical property and residual stress of SLM Inconel-718 alloy manufactured by differing island scanning strategy. *Opt. Laser Technol.* **2015**, *75*, 197–206, doi:https://doi.org/10.1016/j.optlastec.2015.07.009.
12. Blackwell, P. L. The mechanical and microstructural characteristics of laser-deposited IN718. *J. Mater. Process. Technol.* **2005**, *170*, 240–246, doi:http://dx.doi.org/10.1016/j.jmatprotec.2005.05.005.
13. Qi, H.; Azer, M.; Ritter, A. Studies of Standard Heat Treatment Effects on Microstructure and Mechanical Properties of Laser Net Shape Manufactured INCONEL 718. *Metall. Mater. Trans. A* **2009**, *40*, 2410–2422, doi:10.1007/s11661-009-9949-3.
14. Cao, G. H.; Sun, T. Y.; Wang, C. H.; Li, X.; Liu, M.; Zhang, Z. X.; Hu, P. F.; Russell, A. M.; Schneider, R.; Gerthsen, D.; Zhou, Z. J.; Li, C. P.; Chen, G. F. Investigations of γ′, γ″ and δ precipitates in heat-treated Inconel 718 alloy fabricated by selective laser melting. *Mater. Charact.* **2018**, *136*, 398–406, doi:https://doi.org/10.1016/j.matchar.2018.01.006.

© European Powder Metallurgy Association (EPMA)